Electronic Supplementary Material (ESI) for New Journal of Chemistry.

Support information

Sensor	Detection limit	Responding time	selectivity	Remarks
RSC Advances, 2017, **7**, 20369-20372	7.8×10^{-10} M	80min	very high selectivity	CH_3CN-PBS (1 : 1, v/v)
Analyst (Cambridge, United Kingdom), 2016, **141**, 2376-2379	2.1×10^{-9} M	30min	very high selectivity	PBS (10 mM, pH = 7.4)
Analyst (Cambridge, United Kingdom), 2013, **138**, 1564-1569.	no data	20min	interference of Au^{3+} and Cu^{2+}	CH_3CN-H_2O (1 : 1, v/v)
RSC Advances, 2016, **6**, 43539-43542	3.4×10^{-7} M	real-time detection	slight interference of Cu^{2+}	CH_3CN-H_2O (4 : 1, v/v)
Analyst (Cambridge, United Kingdom), 2016, **141**, 832-835	5.5×10^{-8} M	real-time detection	interference of Au^{3+} and Cr^{3+}	pure water
Analytical Chemistry (Washington, DC, United States), 2015, **87**, 4503-4507	2.3×10^{-7} M	real-time detection	very high selectivity	EtOH-PBS (1 : 1, v/v)
This work	4.0×10^{-8} M	real-time detection	very high selectivity	EtOH-H_2O (1 : 1, v/v)

Table 1 Comparison with recent reports in the literature. The first three are reactive palladium sensors and the latter four are coordination sensors.

(a)

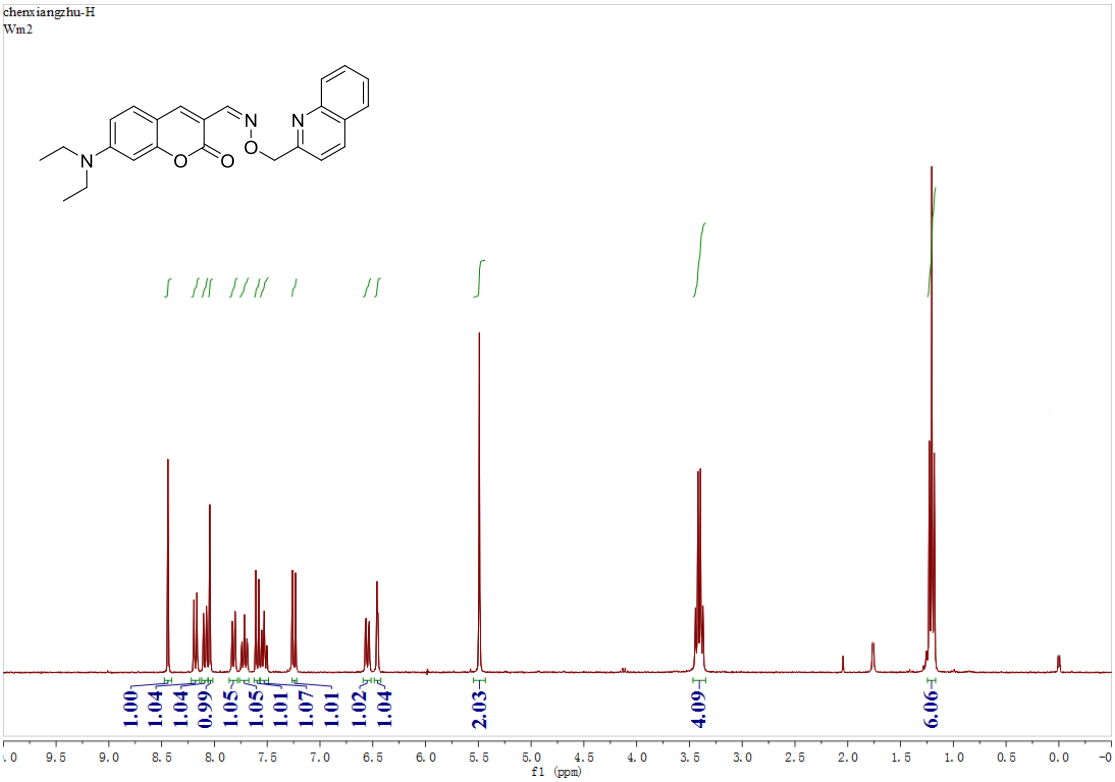
chenxiangzhu-H
Wm2
1.00
1.04
1.04
0.99
1.05
1.05
1.01
1.07
1.01
1.02
1.04
2.03
4.09
6.06
f1 (ppm)

(b)

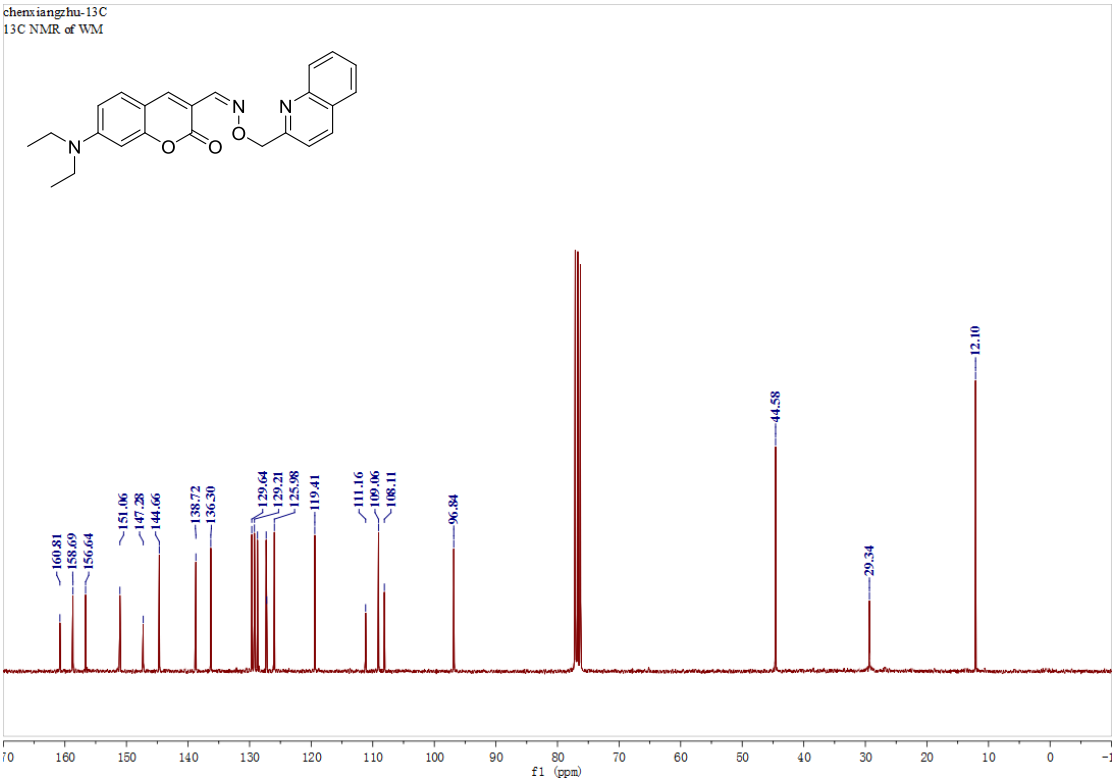
chenxiangzhu-13C
13C NMR of WM
160.81
158.69
156.64
151.06
147.28
144.66
138.72
136.50
129.64
129.21
125.98
119.41
111.16
109.06
108.11
96.84
44.58
29.34
12.10
f1 (ppm)

(c)

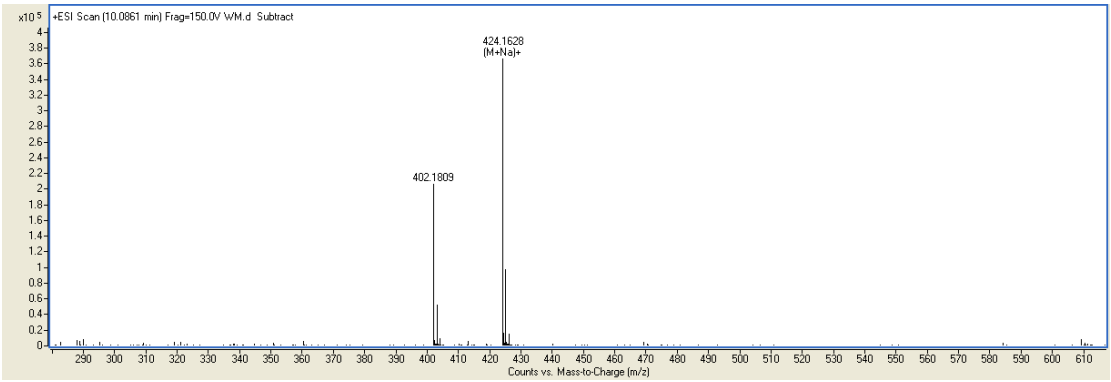

Fig. S1 ^{1}H NMR (a), ^{13}C NMR (b) and HRMS (c) spectra of **P**.

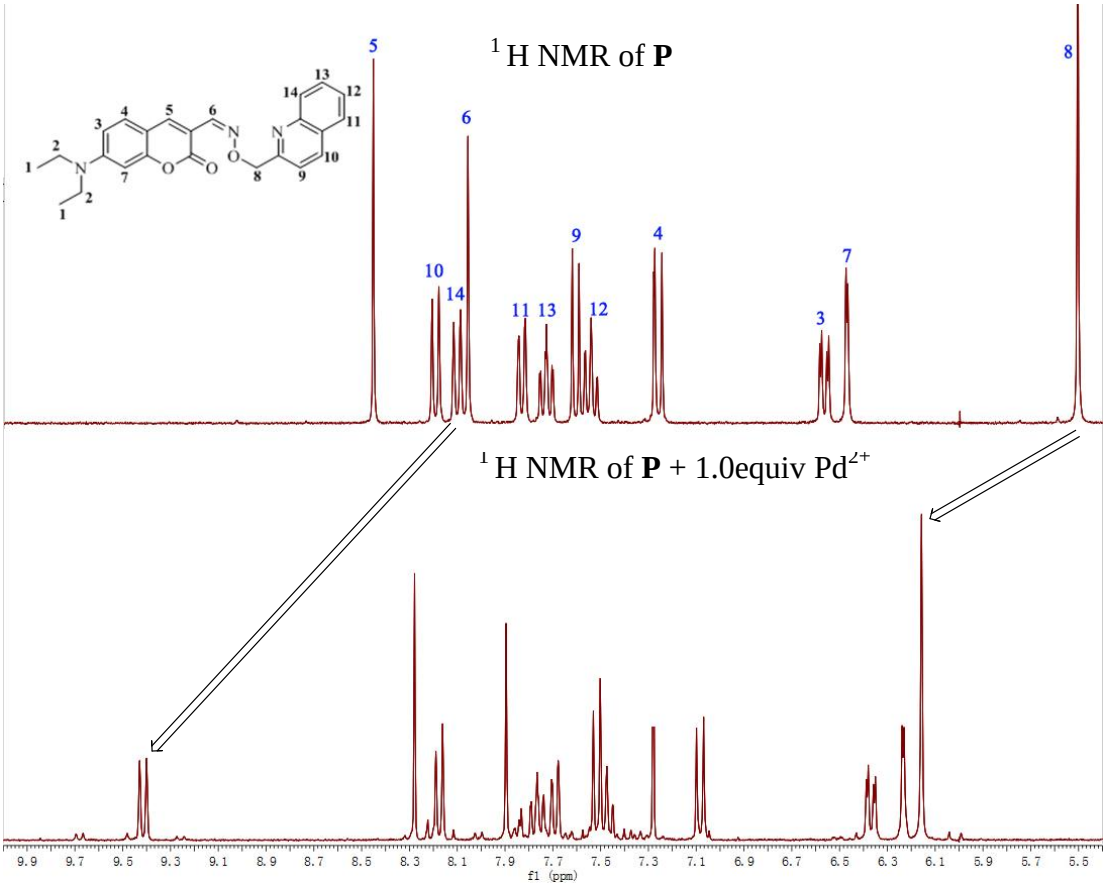

Fig. S2 The nuclear magnetic resonance experiment of **P** (in $CDCl_3$) and 1.0 equiv Pd^{2+} (in Dimethyl sulfoxide-d6)

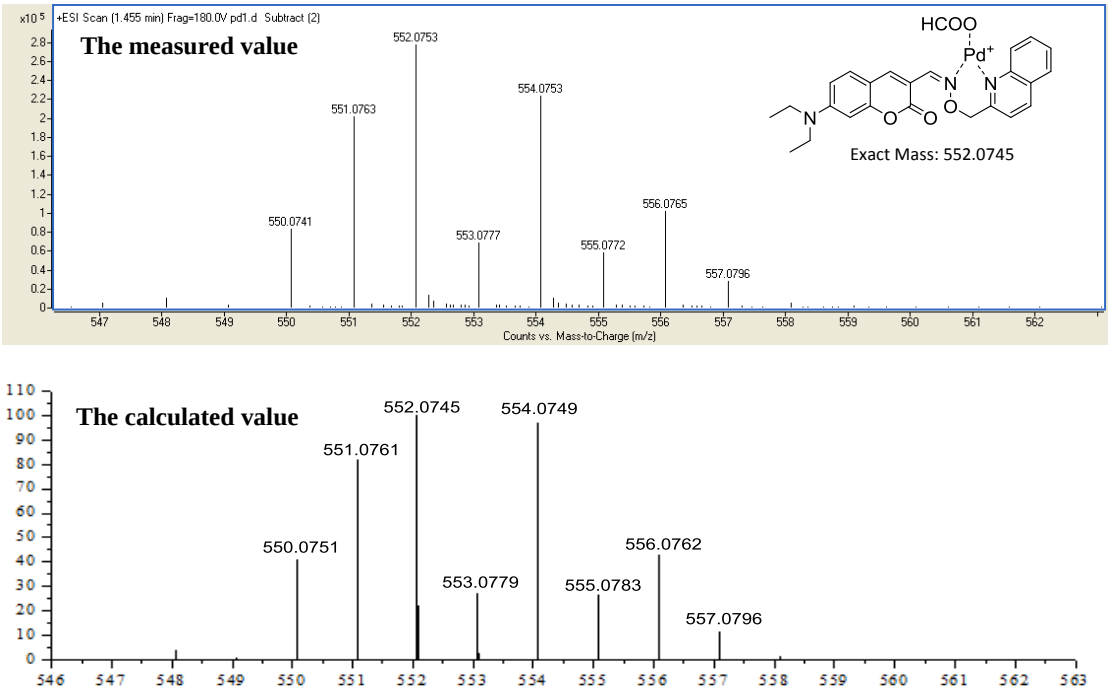

Fig. S3 HRMS spectra of **P** + Pd^{2+}

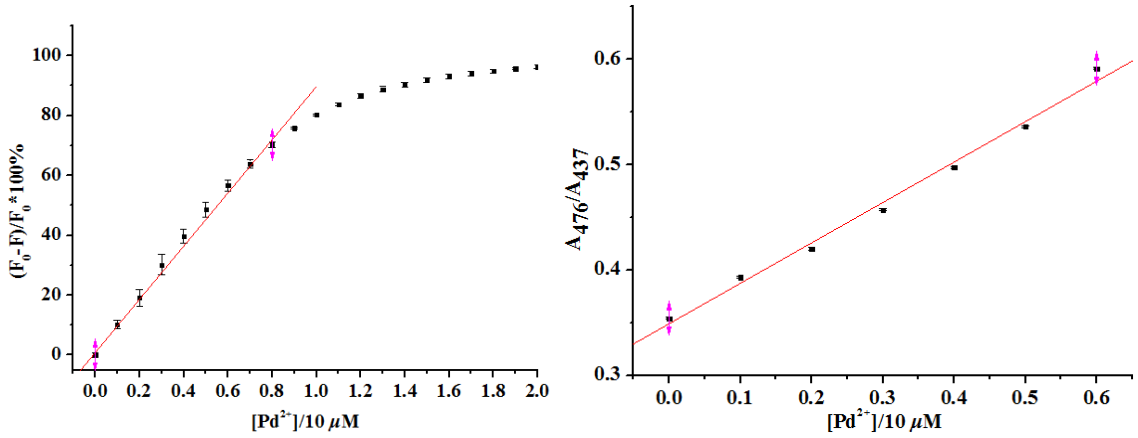

Fig. S4 (a) The percentage decline in fluorescence intensity at 500 nm of **P** (10.0 μM) as a function of the concentration of Pd^{2+} in EtOH-H_2O solution at 25°C. λ_{ex}=437 nm. F_0: the fluorescence intensity at 500 nm of **P** only. F: the fluorescence intensity at 500 nm of **P** in response to the presence of Pd^{2+}. (b) Ratiometric curve of A_{476}/A_{437} as a function of the concentration of Pd^{2+} in EtOH-H_2O solution at 25°C.

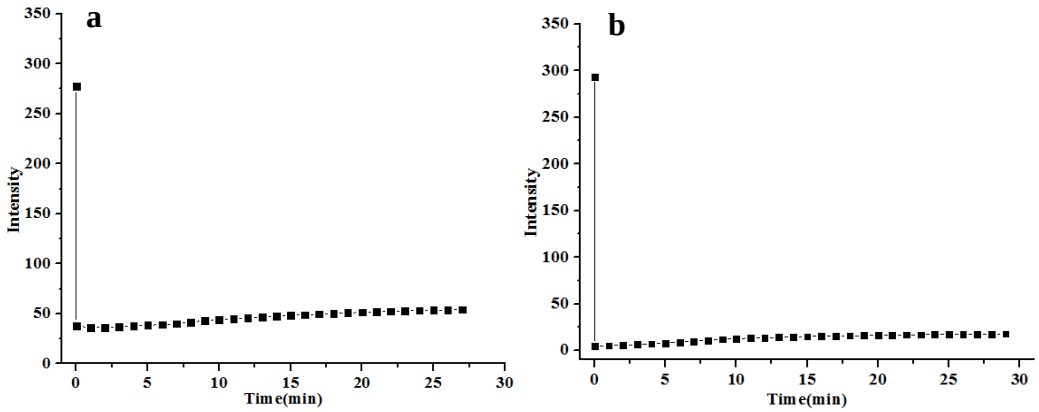

Fig. S5 Time-dependent changes of the fluorescence intensity at 500 nm upon addition of 1.0 (a) or 2.0 (b) equiv of Pd^{2+} in the solution of **P** (10.0 μM). λ_{ex}=437 nm.

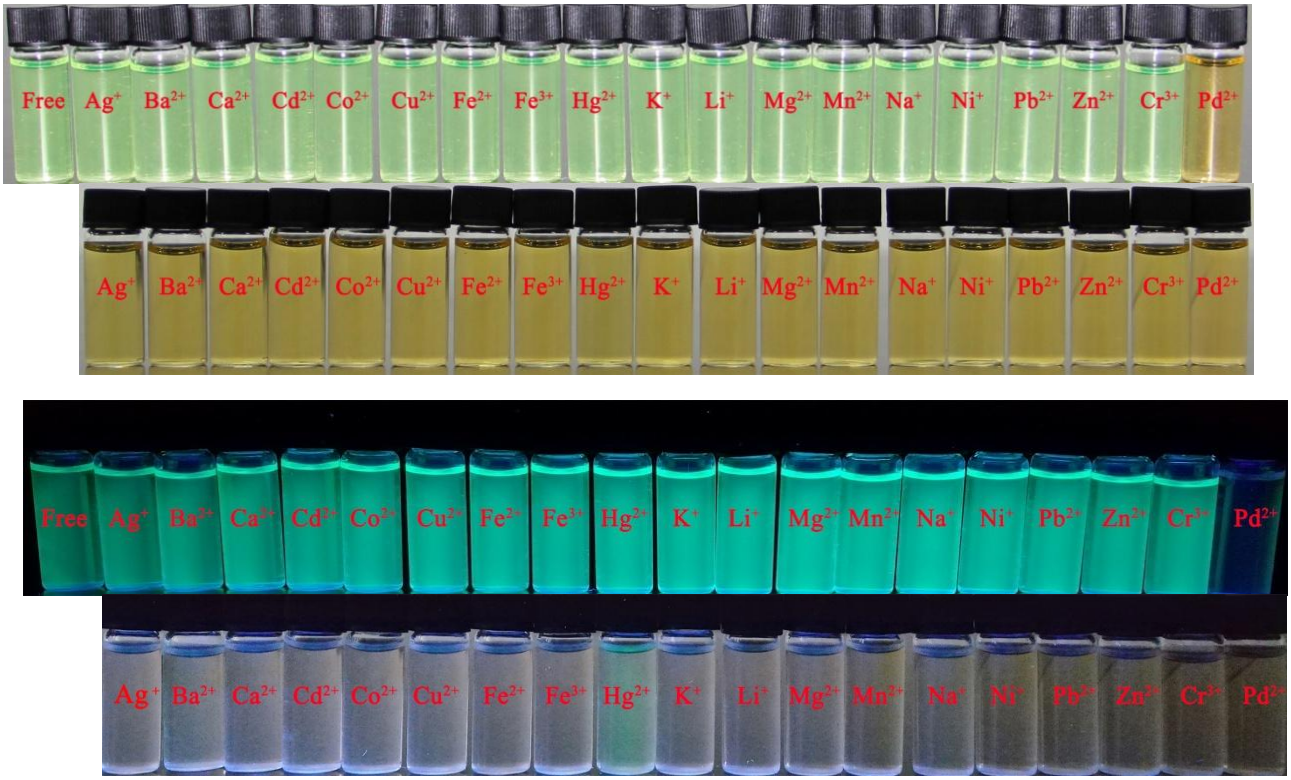

Fig. S6 (a) Color changes and (b) Fluorescence images of of **P** (10.0 μM) in the presence of various metal ions and after further addition of 2.0 equiv of Pd^{2+}. Li^{+}, Mg^{2+}, Mn^{2+}, Na^{+}, Pb^{2+}, Zn^{2+}, Ag^{+}, Ba^{2+}, Ca^{2+}, Cd^{2+}, Co^{2+}, Fe^{2+}, Fe^{3+}, Hg^{2+}, K^{+}, Cu^{2+}, Ni^{+}, Cr^{3+} were added by 5.0 equiv, separately.

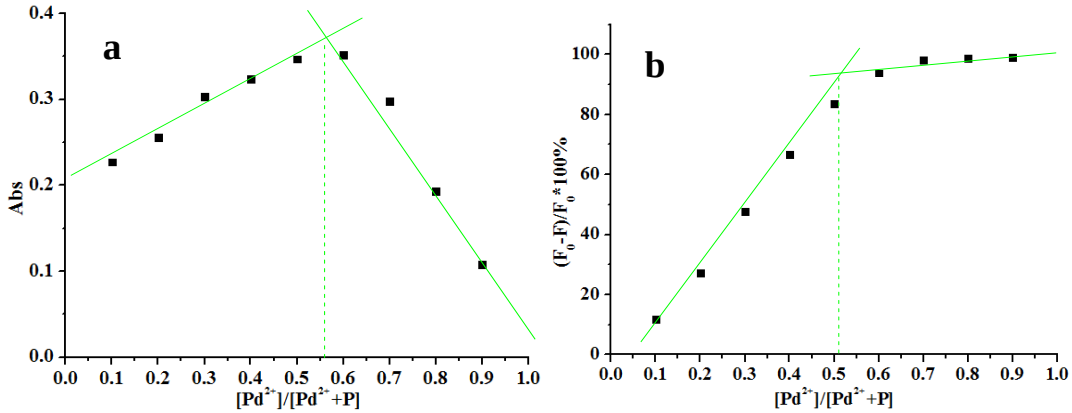

Fig. S7 (a) Job's plot of **P** with Pd^{2+} obtained by UV-Vis absorption spectroscopy (λ=478 nm), the total concentration of **P** and Pd^{2+} is 20 μM. (b) Job's plot of **P** with Pd^{2+} obtained by fluorescence emission spectrometry, the total concentration of **P** and Pd^{2+} is 20 μM. F_0: the fluorescence intensity at 500 nm of **P** only. F: the fluorescence intensity at 500 nm of **P** in response to the presence of Pd^{2+}.

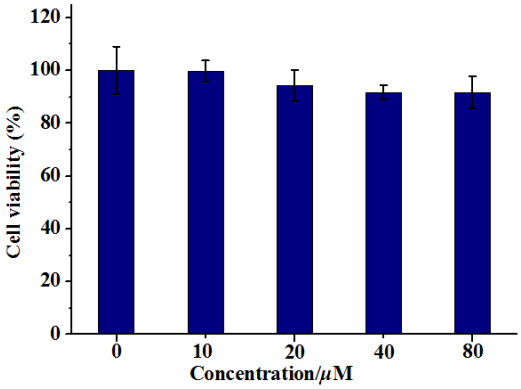

Fig. S8 Cytotoxicity assays of **P** at different concentrations (0 μM, 10 μM, 20 μM, 40 μM, 80 μM) for MARC-145 cells. The cell viabilities were estimated through standard MTT assay. The viability of cells without **P** is defined as 100%. The results are presented as mean ± standard deviation (n = 6).